Supporting Information for

New porphyrin derivatives for phosphate anion sensing in both organic and aqueous media

João M. M. Rodrigues,[a] Andreia S. F. Farinha,[a] Paulino V. Muteto,[b] Sandra M. Woranovicz-Barreira,[a,c] Filipe A. Almeida Paz,[d] Maria G. P. M. S. Neves,[a] Augusto C. Tomé,[a] José A. S. Cavaleiro,[a] M. Teresa S. R. Gomes,[b] Jonathan L. Sessler*[,e] and João P. C. Tomé*[,a]

[a]*QOPNA,* [b]*CESAM and* [d]*CICECO Department of Chemistry, University of Aveiro, 3810-193 Aveiro, Portugal*

[c] *Department of Pharmacy, Federal University of Paraná, 80210-170, Curitiba PR, Brazil*

[e] *Department of Chemistry, 105 E. 24th Street-A5300, The University of Texas at Austin, Austin, TX 78712-1224, USA*

Contents:

1 Experimental Section

1.1 General information

^{1}H, ^{13}C, and ^{19}F solution NMR spectra were recorded on a *Bruker Avance-300* spectrometer at 300.13, 75.47 and 282.38 MHz, respectively. Tetramethylsilane was used as internal reference. HRMS spectra were recorded on VG *AutoSpec-M* spectrometer; using chloroform and methanol as solvent, with 3-nitrobenzyl alcohol (NBA) as matrix. Absorption spectra were recorded in chloroform using a *Shimadzu UV-2501-PC*. Analytical TLC was carried out on precoated silica gel sheets (Merck, 60, 0.2 mm). Column chromatography was carried out over silica gel (Merck, 230–400 mesh).

1.2 Synthesis

General procedure for the preparation of the $TPPF_{20}$ amino derivatives by microwave irradiation: Into a small vial were added 50 mg of 5,10,15,20-tetrakispentafluorophenylporphyrin (51.3 μmol) and 10 equiv. of the chosen amine derivative in ***N***-methyl-2-pyrrolidone (NMP, 0.5 mL). The closed vial was irradiated in a microwave oven (800 W, 1 bar, 200 ºC, Mileston, MicroSYNTH) for 3 min intervals until no starting material could be seen by TLC, usually between 3 to 5 times (9 to 15 min). After that, the solvent was removed by placing under a nitrogen flow. The crude mixture was redissolved in CH_2Cl_2/MeOH (95:5) and washed with an aqueous $KHCO_3$ solution. The organic layer was dried (Na_2SO_4) and the solvent removed under reduced pressure. The desired products were then directly crystalized or purified by column chromatography over silica gel. Typical yields were over 70%.

meso-Tetrakis[4-(2-aminoethylamino)-2,3,5,6-tetrafluorophenyl]porphyrin (1). In a small vial, was dissolved **$TPPF_{20}$** (50.0 mg, 51.3 μmol) and an excess of ethane 1,2-diamine (3.44 mL, 10 equiv.) in NMP (0.5 mL). The reaction mixture was irradiated for 3 x 3 min (9 min). After the workup described above, the product was directly crystalized from $CHCl_3$/MeOH and obtained in 80.8% (41.2 mg) yield. **^{1}H NMR** (DMSO-d_6, in ppm): δ -3.11 (s, 2H, NH), 3.06 (t, J = 6.3 Hz, 8H, CH_2), 3.68 (d, J = 5.8 Hz, 8H, CH_2), 6.52 (s, 4H, NH-PhF_4), 9.24 (s, 8H, β-H); **^{1}H NMR** ($CDCl_3$/DMSO-d_6, in ppm): δ -2.94 (s, 2H, NH), 3.15-3.27 (m, 8H, CH_2), 3.82 (d, J = 5.4 Hz, 8H, CH_2), 6.74 (s, 4H, NH-PhF_4), 9.02 (s, 8H, β-H). **^{19}F NMR** (DMSO-d_6, in

ppm): δ -166.63 (d, *J* = 18.7 Hz, 8F, *o*-F), -184.35 (d, *J* = 18.7 Hz, 8F, *m*-F). **^{13}C NMR** (DMSO-d_6, in ppm): δ 19.2, 28.5, 33.2, 45.2-45.7, 104.2-104.8, 129.7-129.9, 132.1-132.3, 134.8-135.1, 138.0-138.2, 144.7-144.8, 147.9-148.3, 158.0. **UV-Vis** ($CHCl_3$), λ_{max} (log ε): 421 (5.23), 512 (4.18), 587 (3.68), 656 (3.68). **HRMS-ESI:** Calculated for $C_{52}H_{39}F_{16}N_{12}$ $[M+H]^+$ 1135.31597; found 1135.31798.

***meso*-Tetrakis[4-(*N*-tosylethylenediamine)-2,3,5,6-tetrafluorophenyl]porphyrin (2).** In a small vial, was dissolved **TPPF$_{20}$** (50 mg, 51.3 μmol) and an excess of *N*-tosylethylenediamine (110.0 mg, 10 equiv.) in NMP (0.5 mL). The reaction mixture was irradiated for 4 x 3 min (12 min in total). After the workup described above, the product was purified by column chromatography over silica gel using CH_2Cl_2/MeOH (95:5) as the eluent. The product was crystallized from MeOH/H_2O and obtained in 71.8% (63.2 mg) yield. **^{1}H NMR** (DMSO-d_6, in ppm): δ -3.13 (s, 2H, NH), 2.36 (s, 12H, Ts-CH_3), 3.18 (dd, *J* = 12.3, 6.1 Hz, 8H, CH_2), 3.62-3.65 (m, 8H, CH_2), 6.47 (s, 4H, NH-PhF_4), 7.47 (d, *J* = 8.2 Hz, 8H, Ts-*o*-H), 7.81 (d, *J* = 8.2 Hz, 8H, Ts-*m*-H), 7.89 (t, *J* = 5.9 Hz, 4H, NH-Ts), 9.22 (s, 8H, *β*-H). **^{1}H NMR** ($CDCl_3$/DMSO-d_6, in ppm): δ -2.92 (s, 2H, NH), 2.38 (s, 12H, Ts-CH_3), 3.31 (dd, *J* = 10.5, 5.5 Hz, 8H, CH_2), 3.71-3.79 (m, 8H, CH_2), 5.44 (s, 4H, NH-PhF_4), 7.38 (d, *J* = 8.1 Hz, 8H, Ts-*o*-H), 7.48 (t, *J* = 5.7 Hz, 4H, NH-Ts), 7.86 (d, *J* = 8.3 Hz, 8H, Ts-*m*-H), 8.97 (s, 8H, *β*-H). **^{19}F NMR** (DMSO-d_6, in ppm): δ -166.65 (d, *J* = 18.8 Hz, 8F, *o*-F), -183.77 (d, *J* = 18.8 Hz, 8F, *m*-F). **^{13}C NMR** (DMSO-d_6, in ppm): δ 21.0, 40.8-41.9, 43.3, 44.4, 104.5-105.0, 126.6, 129.4-129.8, 131.8-132.3, 135.0-135.3, 137.7, 142.7, 144.6-144.9, 147.7-147.9. **UV-Vis** ($CHCl_3$), λ_{max} (log ε): 421 (5.49), 511 (4.35), 586 (3.86), 653 (3.26). **HRMS-ESI:** Calculated for $C_{80}H_{63}F_{16}N_{12}O_8S_4$ $[M+H]^+$ 1751.35137; found 1751.35098; Calculated for $C_{80}H_{64}F_{16}N_{12}O_8S_4$ $[M+2H]^{2+}$ 876.17932; found 876.17862

***meso*-Tetrakis[4-(*N*-isopropyletilenediamine)-2,3,5,6-tetrafluorophenyl]porphyrin (3).** In a small vial, **TPPF$_{20}$** (50.0 mg, 51.3 μmol) and an excess of *N*-isopropylethane-1,2-diamine (63 μL, 10 equiv.) were dissolved in NMP (0.5 mL). The reaction mixture was irradiated for 5 x 3 min (15 min in total). After the workup, the product was directly crystallized from a mixture of $CHCl_3$/MeOH in 83.2% (55.8 mg) yield. **^{1}H NMR** (DMSO-d_6, in ppm): δ -3.12 (s, 2H, NH), 0.78-0.86 (m, 4H, CH), 1.17 (d, *J* = 6.3 Hz, 24H, CH_3), 3.05 (d, *J* = 5.0 Hz, 8H, CH_2), 3.73 (d, *J* = 5.0 Hz, 8H, CH_2), 6.49 (s, 4H, NH-PhF_4), 9.22 (s, 8H, *β*-H); **^{1}H NMR** ($CDCl_3$/DMSO-d_6, in ppm): δ -2.96 (s, 2H, NH), 0.77-0.91 (m, 4H, CH), 1.55 (d, *J* = 6.2 Hz, 24H, CH_3), 3.56-3.65 (m, 8H, CH_2), 4.04-4.27 (m, 8H, CH_2), 6.46 (s, 4H, NH-PhF_4), 9.04 (s, 8H, *β*-H). **^{19}F NMR**

(DMSO-d_6, in ppm): δ -166.49 (d, J = 18.4 Hz, 8F, *o*-F), -183.09 (d, J = 18.4 Hz, 8F, *m*-F). **^{13}C NMR** (DMSO-d_6, in ppm): 17.2, 19.3, 19.9, 20.5, 21.2, 22.7, 40.8-41.7, 43.6, 45.9, 48.5, 48.7, 79.3, 104.4-104.8, 129.6-129.9, 132.0-132.2, 135.0-135.2, 138.1-138.4, 141.0, 144.5-144.9, 147.6-147.9. **UV-Vis** ($CHCl_3$), λ_{max} (log ε): 421 (5.40), 511 (4.31), 587 (3.81), 655 (3.84). **HRMS-ESI:** Calculated for $C_{64}H_{63}F_{16}N_{12}$ $[M+H]^+$ 1303.50377; found 1303.50460.

Evidence that the compounds were prepared as proposed came initially from ^{1}H NMR spectroscopic analyses. The ^{1}H NMR spectra of all three products are characterized by the expected resonances for the *β*-pyrrolic and the inner NH protons; these appear at δ 9.2 and -3.1 ppm, respectively. The resonances of the ethylene groups, of the amino arms, appear between 3 and 4 ppm, while the arylamino protons (Ar-NH) appears as broad singlets at δ 6.5 ppm. In the case of Por **2**, the CH_2NHR' signals appear at δ 7.89 ppm in the form of a triplet. Additionally, the spectrum of **2** contains a singlet at δ 2.36 ppm and two doublets at 7.47 and 7.81 that are ascribed to the tosyl groups. Likewise, the spectrum of **3** contains a multiplet at δ 0.78-0.86 ppm and one doublet at δ 1.17 ppm, that originate in the CH and CH_3 protons of the isopropyl groups, respectively. The ^{19}F NMR spectra of **1-3** are consistent with the presence of four aryl C-F substituents. Moreover, in **1-3** the signal at δ -172 ppm, corresponding to the four *para*-fluorine atoms, is absent.

Further support for the proposed structures came from mass spectrometric analyses and, in the case of **1**, an X-ray structure of a derivative. Experimental data corresponding to this structure is provided later on in this Supporting Information file.

1.3 UV-Vis spectroscopic titrations involving anion salts and the neutral forms of 1-3

Anion binding studies were carried using UV-Vis spectroscopy in chloroform. The titrations were performed using a stock solution of each porphyrin with the spectra being recorded following the addition of aliquots of a stock anion solution. All anions were studied as the corresponding TBA salts. The variation in the absorbance at the Soret band caused by the consecutive addition of the anion was used to determine the affinity constants. The spectral changes were fit using nonlinear least-squares procedures using the following equations for 1:1 and 1:2 binding, respectively: $(\Delta A/l)=([Por]x(K_{11}.\Delta\varepsilon_{11}.[anion])/(1+K_{11}.[anion])$ and $(\Delta A/l)=([Por]x(K_{11}.\Delta\varepsilon_{11}.[anion]+K_{11}.K_{12}.\Delta\varepsilon_{12}[anion]^2)/(1+K_{11}.[anion]+K_{11}.K_{12}.[anion]^2$.[1]

The experiments were conducted in $CHCl_3$ at 22 ºC. Measurements were repeated 2-3 times and found to be reproducible within 15-20%.

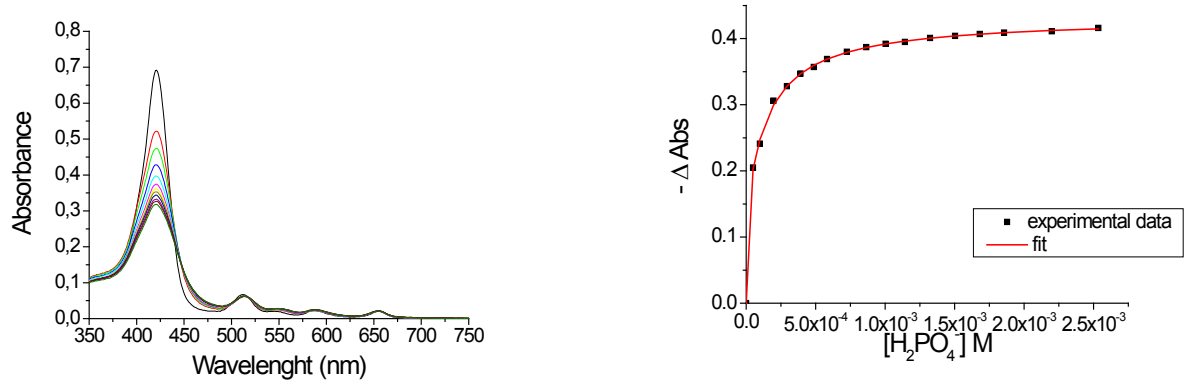

a) Porphyrin **1** titrated with $H_2PO_4^-$ as the TBA (tetrabutylammonium) salt (left) and plot of the experimental data and corresponding fit to a 1:1 binding model at 422 nm (right).

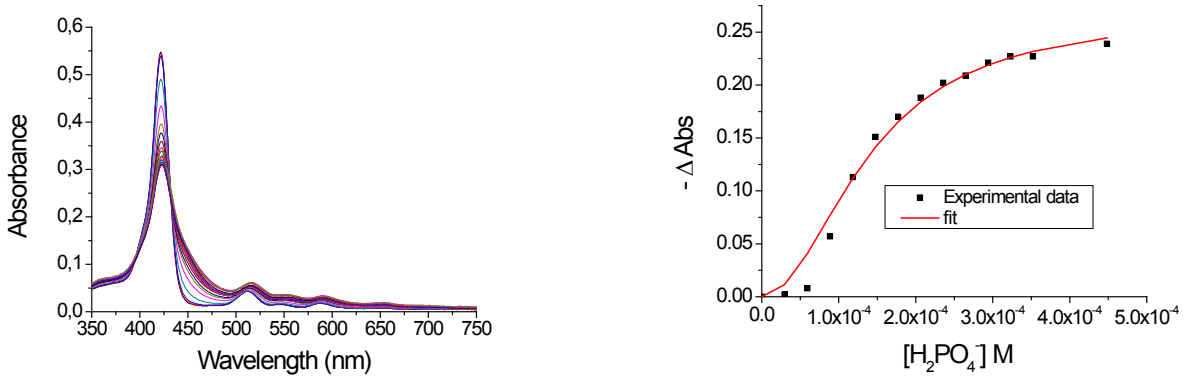

b) Porphyrin **2** titrated with $H_2PO_4^-$ (left) and plot of the experimental data and corresponding fit to a 1:2 binding model at 422 nm (right).

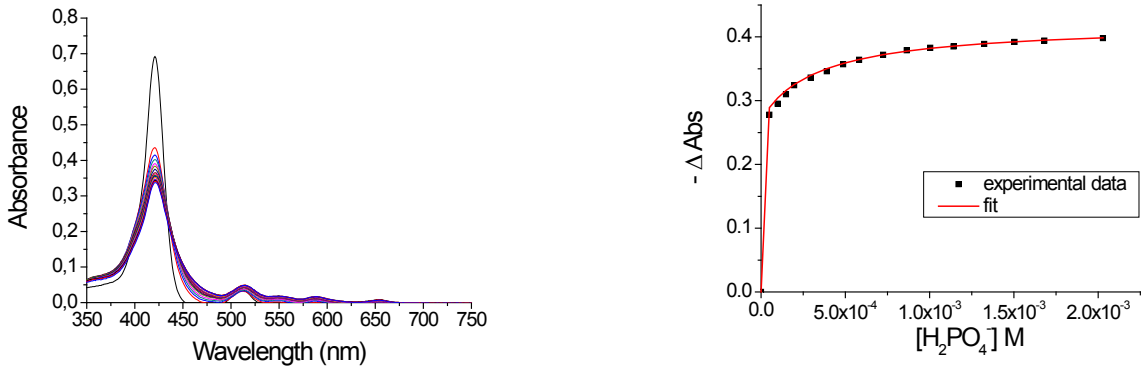

c) Porphyrin **3** titrated with $H_2PO_4^-$ (left) and plot of the experimental data and corresponding fit to a 1:2 binding model at 422 nm (right).

Figure SI 1: Changes in the absorption spectra of porphyrins **1-3** seen upon the addition of $H_2PO_4^-$ (TBA salt) in $CHCl_3$. Also shown are the calculated fits of the experimental titration data using a 1:1 or 2:1 model as appropriate.

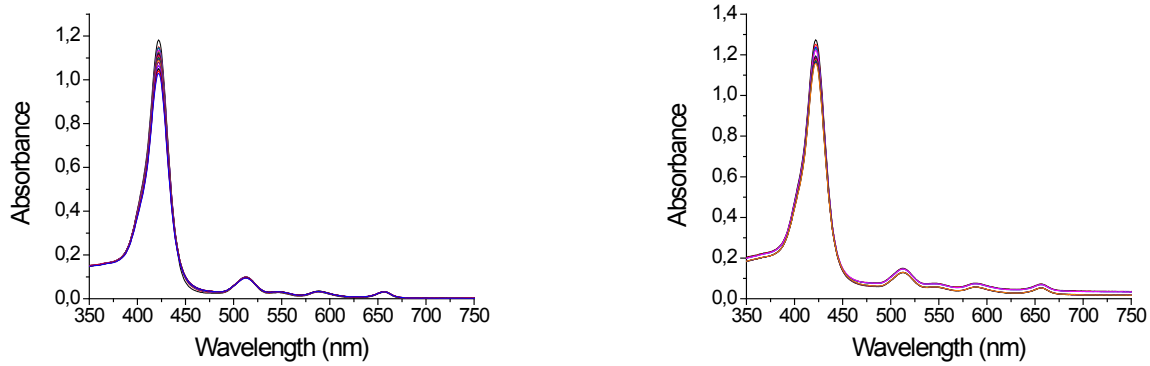

a) Porphyrin **1** titrated with AcO^- (right) and F^- (left).

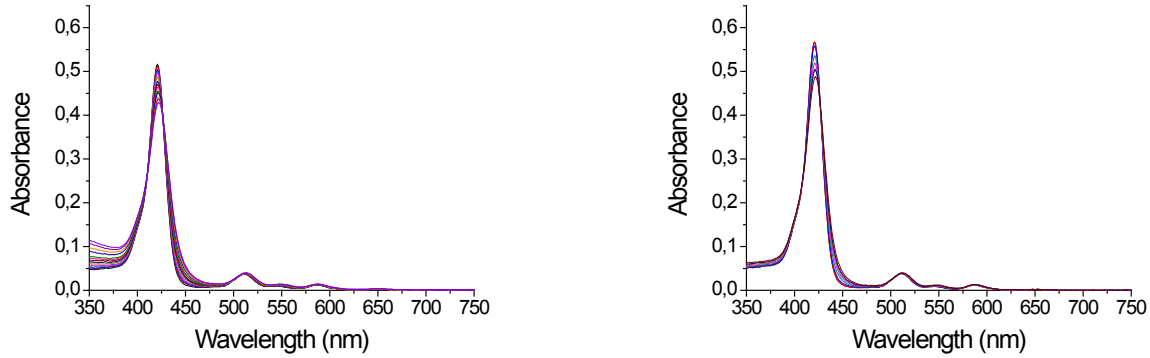

b) Porphyrin **2** titrated with AcO^- (right) and F^- (left).

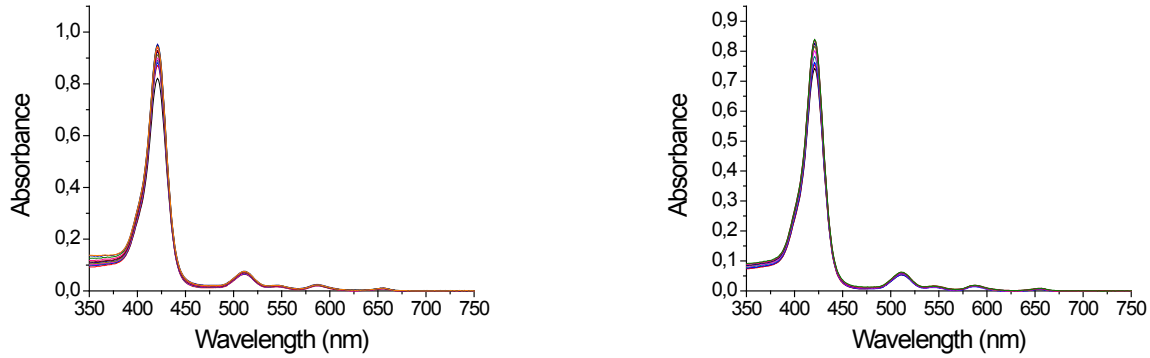

c) Porphyrin **3** titrated with AcO^- (right) and F^- (left)

Figure SI 2: Example of the changes in the absorption spectra for porphyrins **1-3** seen upon addition of the addition of various anions (as the corresponding TBA salts) in $CHCl_3$.

1.4 UV-Vis spectroscopic titrations involving the protonated forms of porphyrins 1-3

The secondary amine of sensors **1**–**3** were protonated by the addition of 4 equiv. of trifluoroacetic acid (TFA). Towards this end, 10 mg aliquots of compounds **1-3** were individually dissolved in a mixture of dichloromethane / methanol (85/15) in a small flask. Then, 4 equiv. of TFA were added to protonate the external amine group. The mixture was stirred for 5 min. and then the solvent was evaporated off under reduced pressure.

To confirm that protonation of the inner nitrogen atoms does not occur under these conditions, one or two drops of conc. HCl were added to test solutions. This caused the solutions to change color immediately, going from red to green as typically occurs when porphyrins such as **1-3** are subject to ring-centered protonation. Dramatic changes in the UV-Vis spectra were also seen as shown in Figure SI 3.

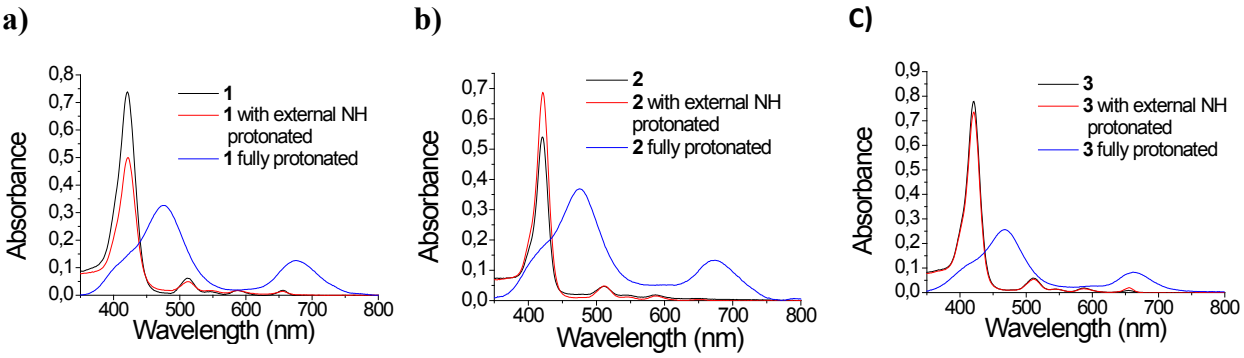

Figure SI 3: Changes in the absorption spectra observed upon protonation of the internal pyrrolic nitrogen atoms with an excess of HCl. The individual figures are as follows: **a) 1**; **b) 2** and **c) 3** in chloroform.

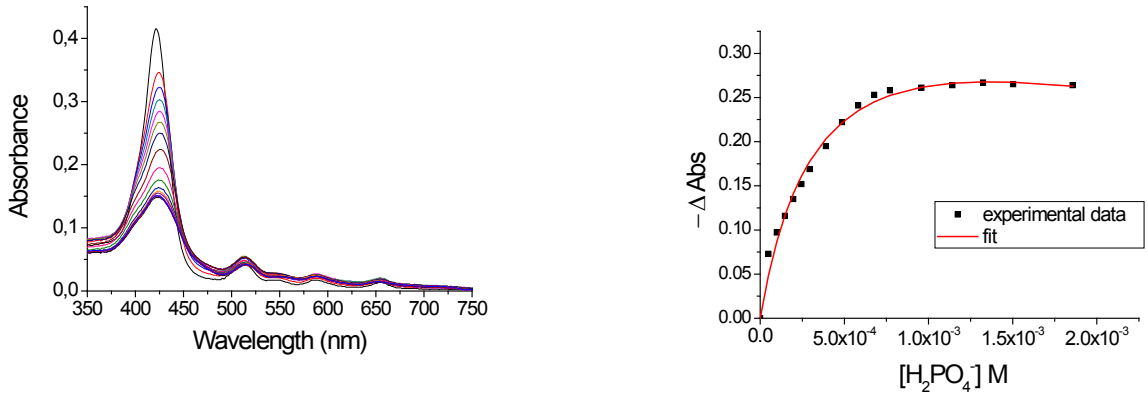

a) Protonated porphyrin **1** titrated with $H_2PO_4^-$ as its TBA salf (right) and plot of the experimental data and corresponding fit to a 1:2 binding model at 422 nm (left).

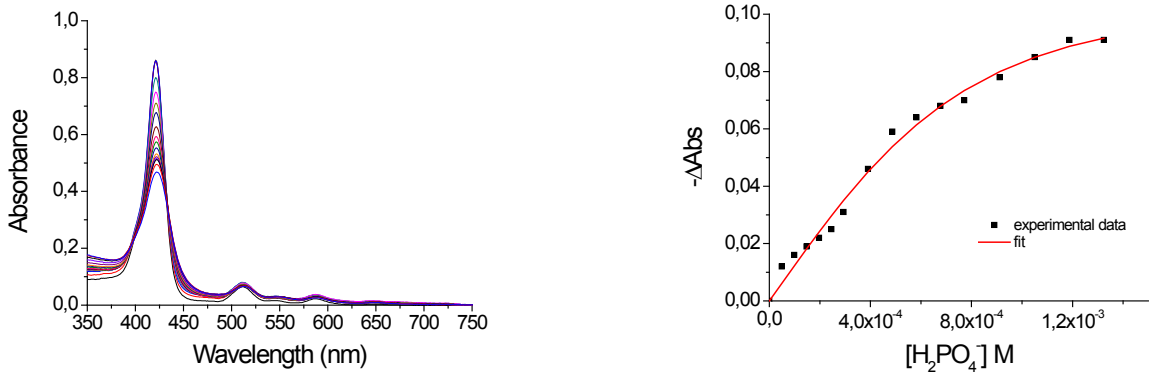

b) Protonated porphyrin **2** titrated with $H_2PO_4^-$ (right) and plot of the experimental data and corresponding fit to a 1:2 binding model at 422 nm (left).

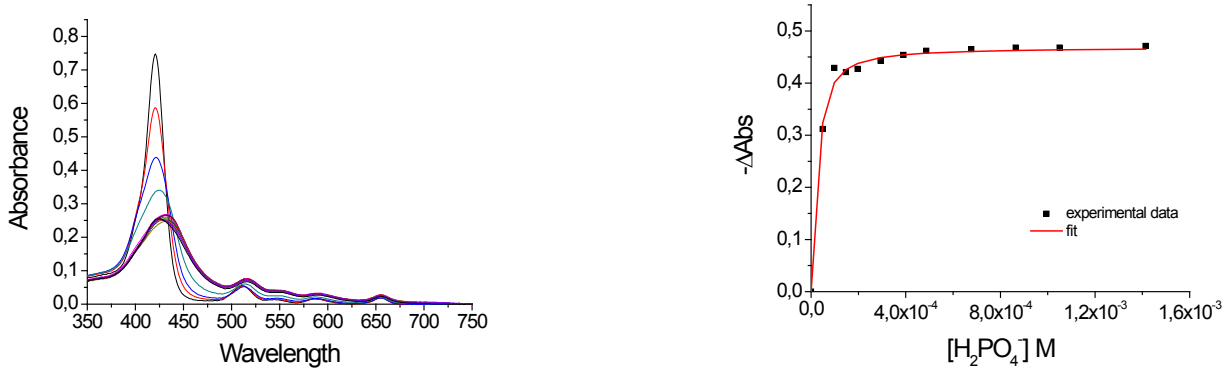

c) Protonated porphyrin **3** titrated with $H_2PO_4^-$ (right) and plot of the experimental data and corresponding fit to a 1:2 binding model at 422 nm (left).

Figure SI 4: Changes in the absorption spectra of protonated porphyrins **1-3** seen upon the addition of $H_2PO_4^-$ (TBA salt) in $CHCl_3$ and the corresponding fits of the titration data to standard binding models.

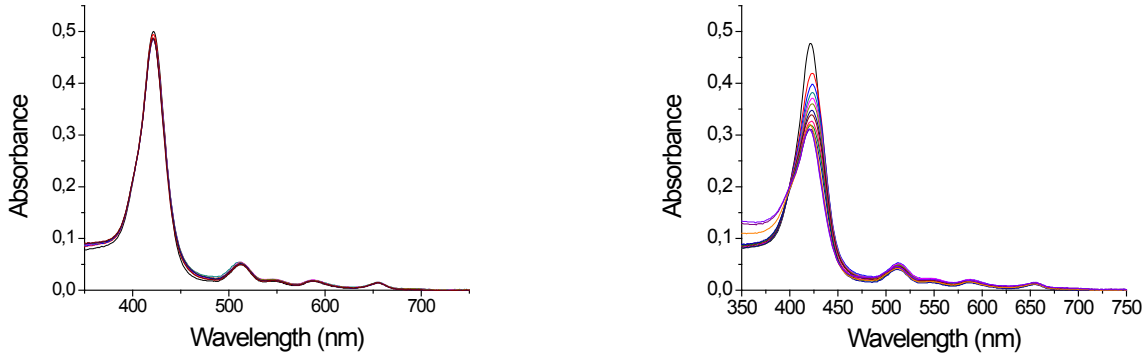

a) Protonated porphyrin **1** titrated with AcO^- (right) and F^- (left) as the TBA salts.

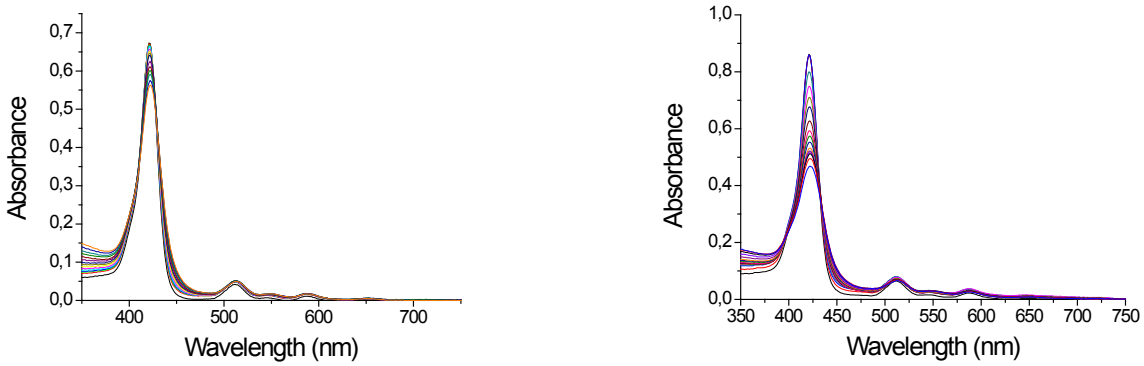

b) Protonated porphyrin **2** titrated with AcO^- (right) and F^- (left) as the TBA salts.

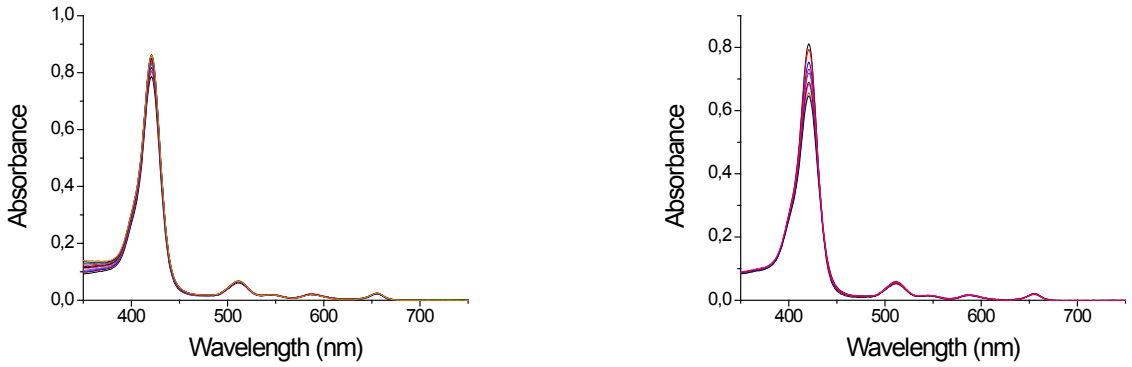

c) Protonated porphyrin **3** titrated with AcO^- (right) and F^- (left)

Figure SI 5: Example of the changes in absorption spectra of the protonated forms of porphyrins **1-3** seen upon the addition of various anions (as the corresponding TBA salts) in $CHCl_3$.

1.5 ^{1}H NMR spectroscopic titration studies involving the neutral or protonated forms of porphyrins 1-3

Anion binding studies conducted using ^{1}H NMR spectroscopy were carried out in $CDCl_3$/DMSO-d_6 (1:1). The titrations were performed using, separately, solutions of both the neutral and protonated* forms of each porphyrin (around 1 mM) and then adding between 0.1 to 2.5 equivalents of the TBA salts of various test anions. The variation of the NH proton signals caused by the addition of the anion was used to infer the main interactions between the species (e.g., hydrogen bonding vs. deprotonation).

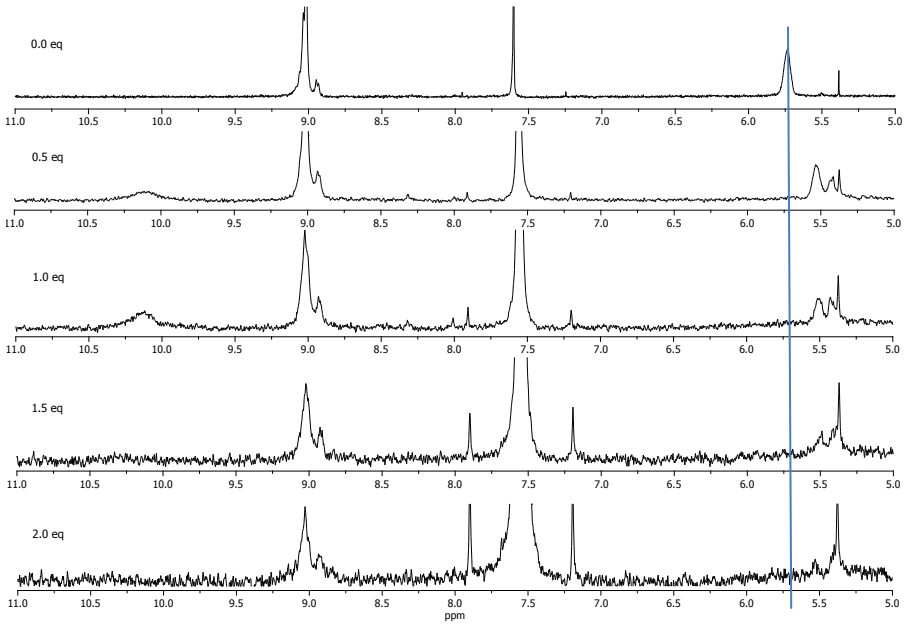

Figure SI 6: Partial ^{1}H NMR spectra of **1** in $CDCl_3$/DMSO-d_6 recorded upon the addition of 0.5 to 2.0 molar equivalents of the $H_2PO_4^-$ anion (as the TBA salt).

* A reliable ^{1}H NMR titration of the protonated form of Por **1** could not be carried out under analogous conditions due to its low solubility in this solvent mixture.

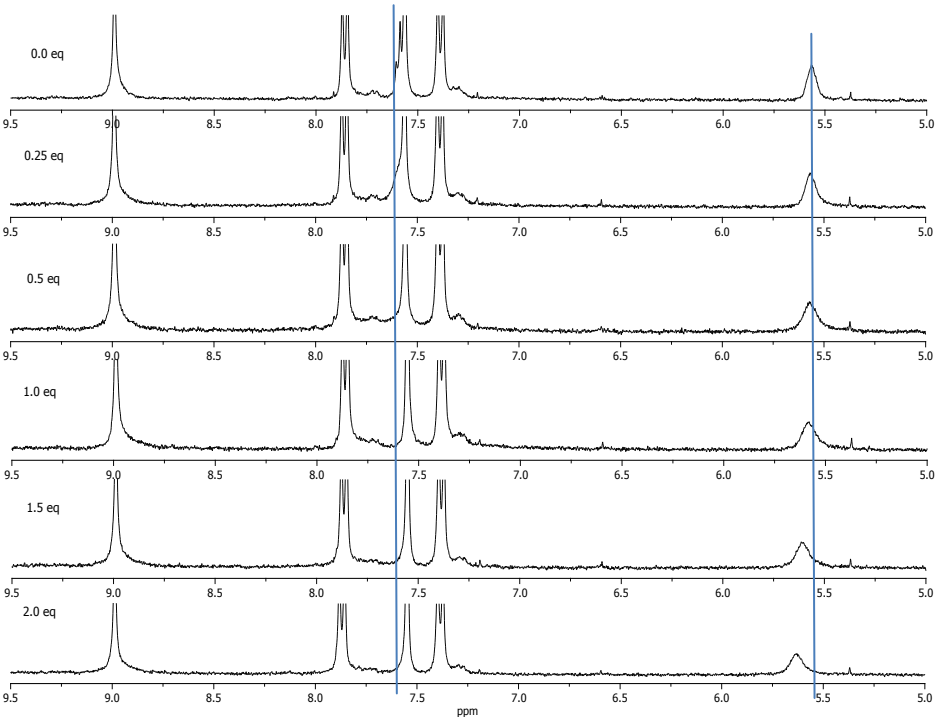

Figure SI 7: Partial ^{1}H NMR spectra of the protonated form of porphyrin **2** recorded in $CDCl_3$/DMSO-d_6 upon the addition of 0.25 to 2.0 molar equivalents of the $H_2PO_4^-$ anion (as the TBA salt).

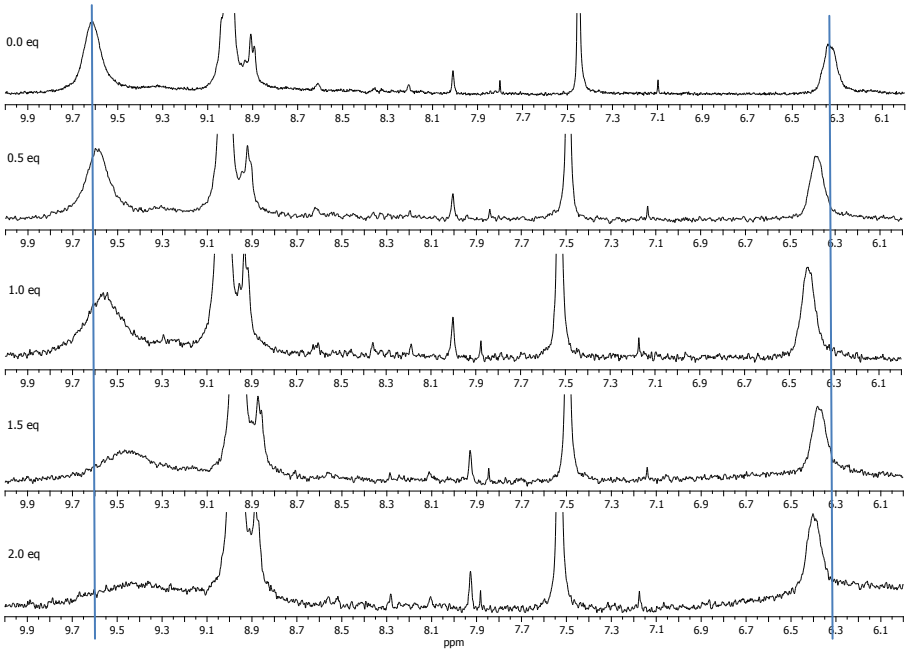

Figure SI 8: Partial ^{1}H NMR spectra of porphyrin **3** in $CDCl_3$/DMSO-d_6 recorded upon the addition of 0.5 to 2.5 molar equivalents of the $H_2PO_4^-$ anion (as the TBA salt).

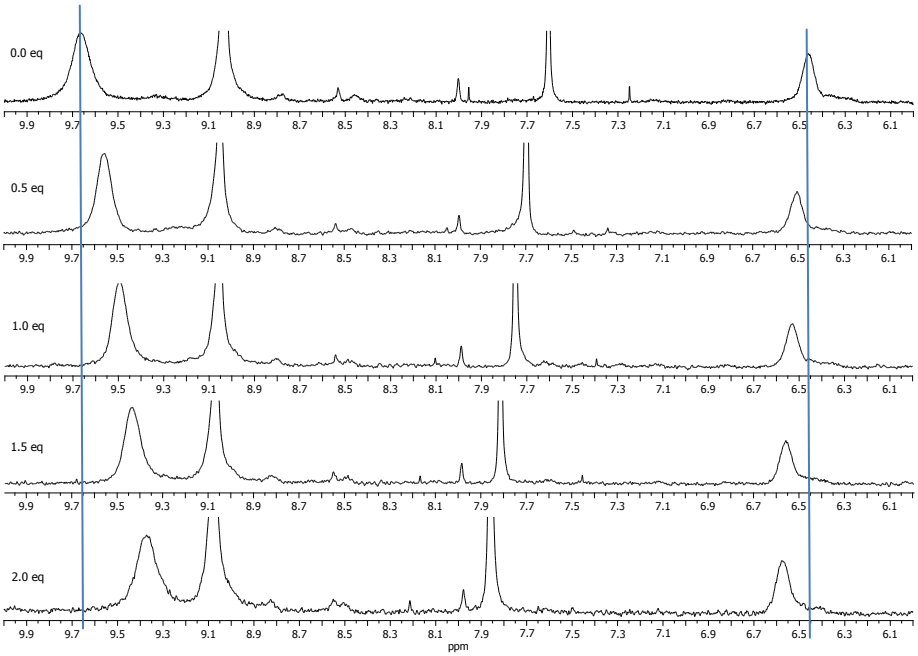

Figure SI 9: Partial ^{1}H NMR spectra of the protonated form of porphyrin **3** recorded in $CDCl_3$/DMSO-d_6 upon the addition of 0.5 to 2.0 molar equivalents of the $H_2PO_4^-$ anion (as the TBA salt).

1.6 Anion-receptor interactions in aqueous medium

Piezoelectric quartz crystals were 9 MHz AT-cut HC-6/U with gold electrodes deposited over a chromium layer (ICM-International Crystal Manufacturing Co, Inc). A spin coater (Süss Delta 10 BM) was used to coat one face of the quartz crystal with a chloroform solution of the selected porphyrin.

Figure SI 10 shows the flow injection analytical system (FIA) with the chemical sensor based on a porphyrin coated piezoelectric quartz crystal. Distilled water with the pH adjusted to a value at which the anion under study is totally ionized (and converted into the desired chemical form) was extruded from the source bottle via use of nitrogen pressure, a technique that assures a constant flow of 0.8 mL mim^{-1}. A standard solution of one of the anions at the chosen pH was injected onto the FIA system. A 0.5 mL of the solution was then carried to the quartz crystal cell by the flowing water stream and, in such a way, was able to contact the coated face of the piezoelectric crystal. The frequency of the quartz crystal was measured by a frequency counter (Leader LF827), and stored on a computer at 1s intervals. The difference between the baseline frequency and the minimum frequency value observed after the anion solution reached the coated quartz crystal was computed.

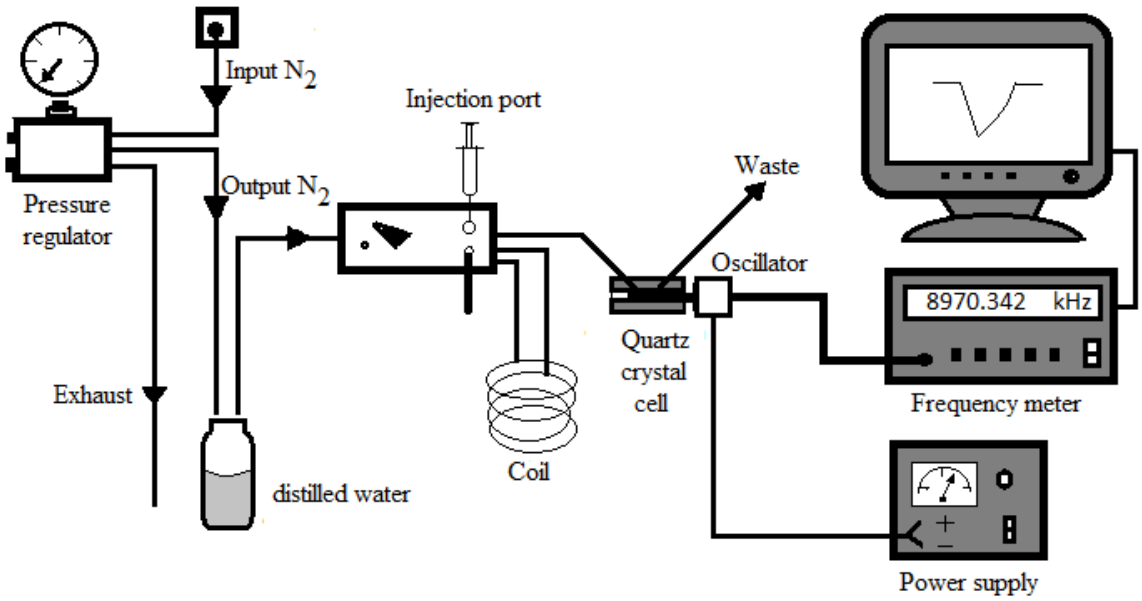

Figure SI 10: Flow injection system containing a piezoelectric quartz crystal coated with porphyrins **1**, **2**, or **3**.

Table SI 1: Selectivity coefficients for the sensor based on Por **1**

	Selectivity coefficients
$K(HPO_4^{2-},AcO^-)$	0.22
$K(HPO_4^{2-},Cl^-)$	0.41
$K(HPO_4^{2-},NO_3^-)$	0.44
$K(HPO_4^{2-},F^-)$	0.48
$K(HPO_4^{2-},HPO_4^{2-})$	1.00

Table SI 2: Selectivity coefficients for the sensor based on Por **2**

	Selectivity coefficients
$K(HPO_4^{2-},AcO^-)$	0.36
$K(HPO_4^{2-},F^-)$	0.48
$K(HPO_4^{2-},NO_3^-)$	0.53
$K(HPO_4^{2-},Cl^-)$	0.55
$K(HPO_4^{2-},HPO_4^{2-})$	1.00

Table SI 3: Selectivity coefficients for the sensor based on Por **3**

	Selectivity coefficients
$K(HPO_4^{2-},AcO^-)$	0.66
$K(HPO_4^{2-},NO_3^-)$	0.86
$K(HPO_4^{2-},F^-)$	0.87
$K(HPO_4^{2-},Cl^-)$	0.94
$K(HPO_4^{2-},HPO_4^{2-})$	1.00

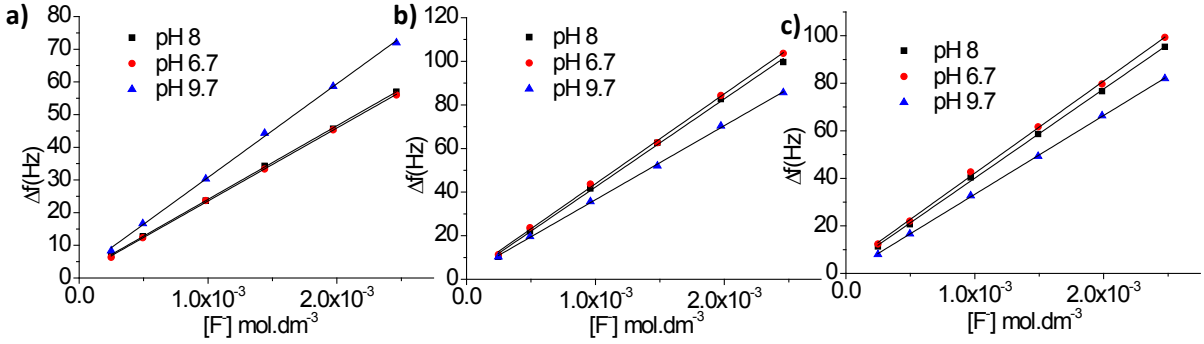

Figure SI 11: Effect of pH on the response of the sensors of this study to the fluoride anion (sodium salt) **a)** Por **1**; **b)** Por **2**; **c)** Por **3**.

1.7 X-Ray structural characterization of the bis-HF complex of the imine derivative of porphyrin 1

A suitable single-crystal was mounted on a Hampton Research CryoLoop using FOMBLIN Y perfluoropolyether vacuum oil (LVAC 25/6) purchased from Aldrich,[2] with the help of a Stemi 2000 stereomicroscope equipped with a Carl Zeiss lenses. Data were collected at 100(2) K on a Bruker X8 Kappa APEX II charge-coupled device (CCD) area-detector diffractometer (Mo Kα graphite-monochromated radiation, λ = 0.71073 Å) controlled by the APEX2 software package,[3] and equipped with an Oxford Cryosystems Series 700 cryostream monitored remotely using the software interface Cryopad.[4] Images were processed using the software package SAINT+,[5] and the data were corrected for absorption by the multi-scan semi-empirical method implemented in SADABS.[6] The structure was solved by the direct methods of SHELXS-97,[7] and refined by full-matrix least squares on F2 using SHELXL-97.[8]

All non-hydrogen atoms were directly located from the difference Fourier maps and successfully refined with anisotropic displacement parameters. Hydrogen atoms associated with N2 and N3 were particularly prominent in the difference Fourier maps and were included in the structure with the N–H distances restrained to 0.95(1) Å and with Uiso = 1.5×Ueq(N). The partially-occupied (50%) hydrogen atom bound to N4 and those attached to carbon were located at their idealised positions and included in the structural model in subsequent refinement cycles in riding-motion approximation with Uiso = 1.2 (aromatic, $–CH_2–$ and CH hydrogen atoms) or 1.5 (for the terminal $–CH_3$ groups and the NH moiety) of Ueq of the parent atom (Figure SI 12).

A chloroform solvent molecule was directly located from the difference Fourier maps but found to be only partially-occupied (50%). Considerable smeared-out electron density was also found in the various empty spaces available throughout the structure. This prevented the sensible location and refinement of additional $CHCl_3$ molecules. Searches for the total potential solvent area using the software package PLATON[9,10] revealed the presence of 16 small cavities accounting for a total internal volume of ca. 2387 $Å^3$ (ca. 14% of the total volume of the unit cell). The original data set was then mathematically treated using the SQUEEZE[11] subroutines in order to remove the contribution of these highly disordered molecules in the solvent-accessible volume. It was estimated that the ca. 15% empty volume would contain ca. 775 unidentified electrons. The calculated solvent-free reflection list was used for additional structural refinement cycles in order to obtain the structural model presented in this manuscript. Further details of this structure may be obtained from the Cambridge Crystallographic Data Centre by quoting CCDC no. 732151.

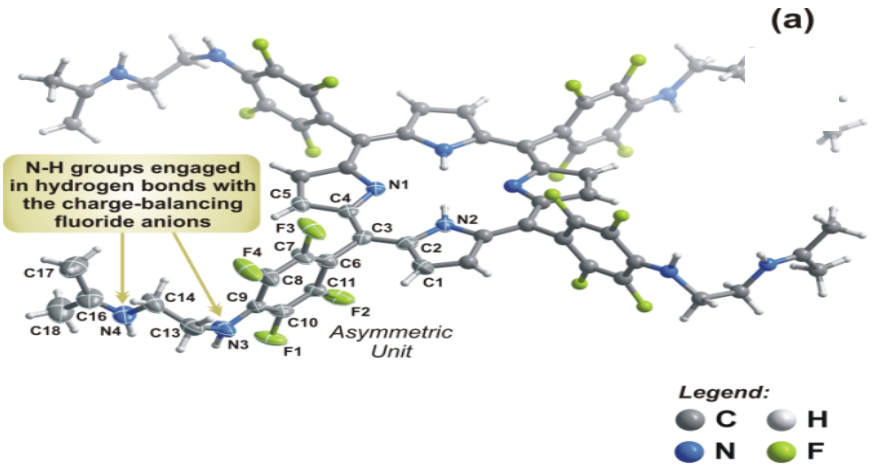

Figure SI 12: Schematic representation of the molecular unit present in the crystal structure corresponding to the diprotonated form of the acetone-derived imine adduct of receptor **1**. Atoms making up the asymmetric unit are represented in the form of thermal ellipsoids drawn at the 50% probability level with the hydrogen atoms as spheres of arbitrary radii.

1.8 NMR spectra and mass spectrometric data for all new compounds

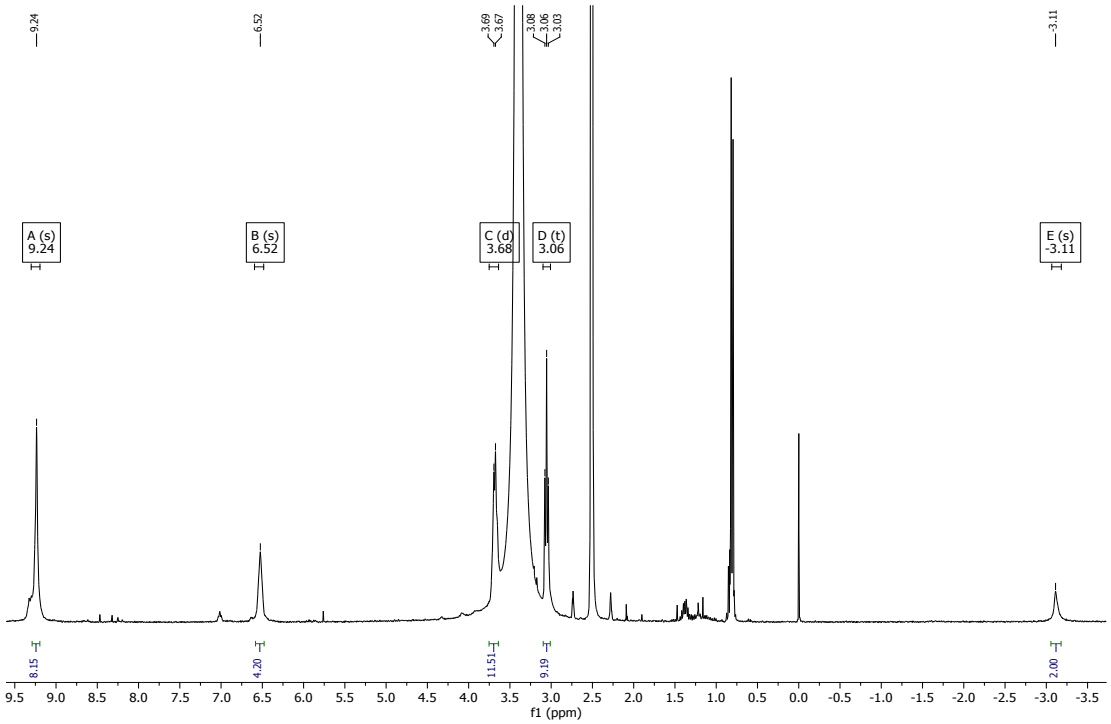

Figure SI 13: ^{1}H NMR spectrum of compound **1** in DMSO-d_6

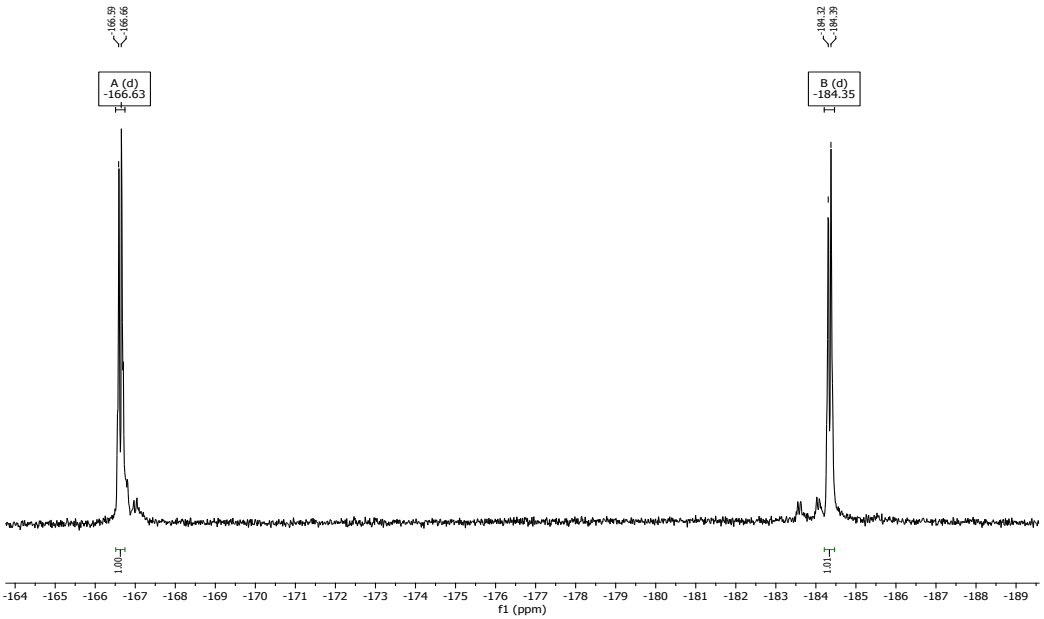

Figure SI 14: ^{19}F NMR spectrum of compound **1** in DMSO-d_6

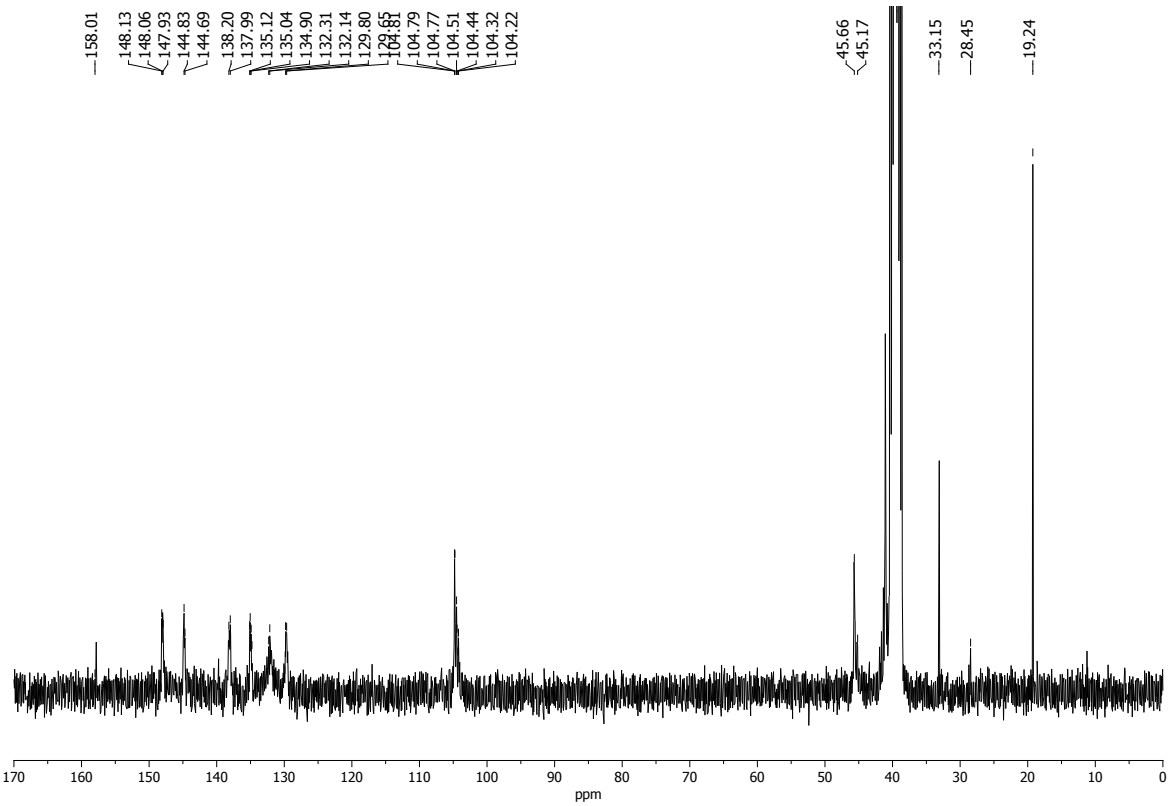

Figure SI 15: ^{13}C NMR spectrum of compound **1** in DMSO-d_6

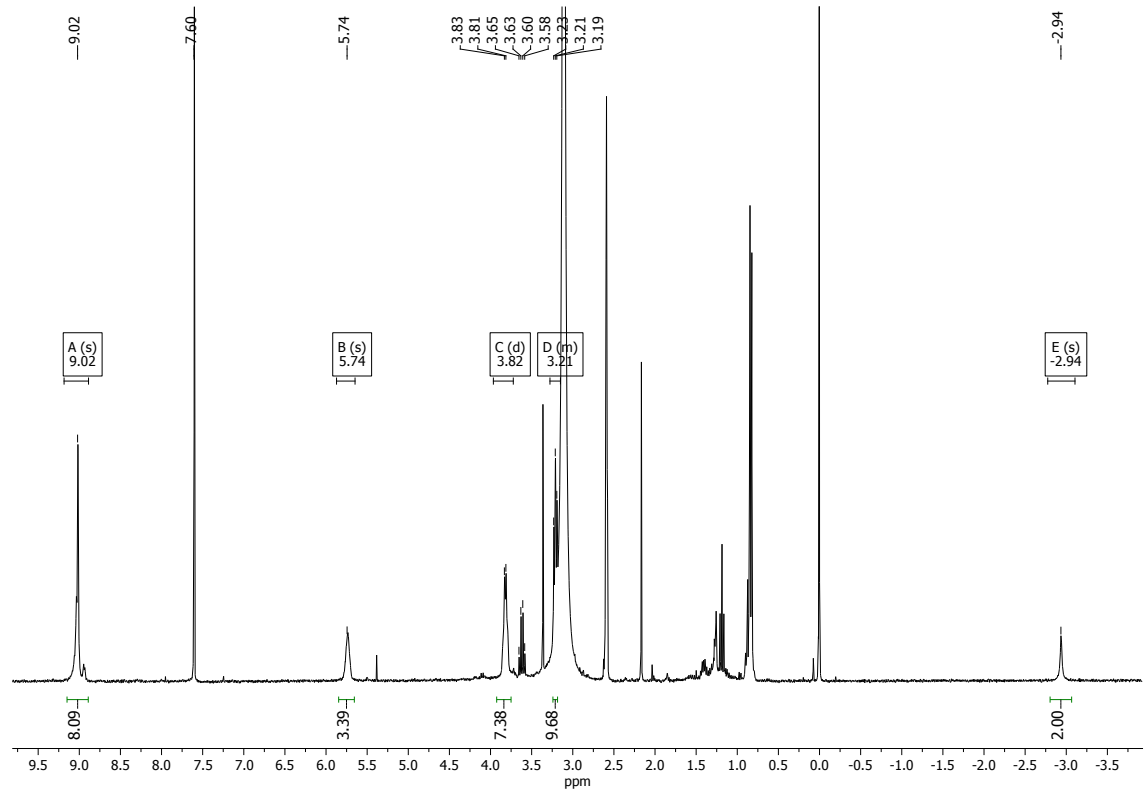

Figure SI 16: ^{1}H NMR spectrum of compound **1** in $CDCl_3$/DMSO-d_6

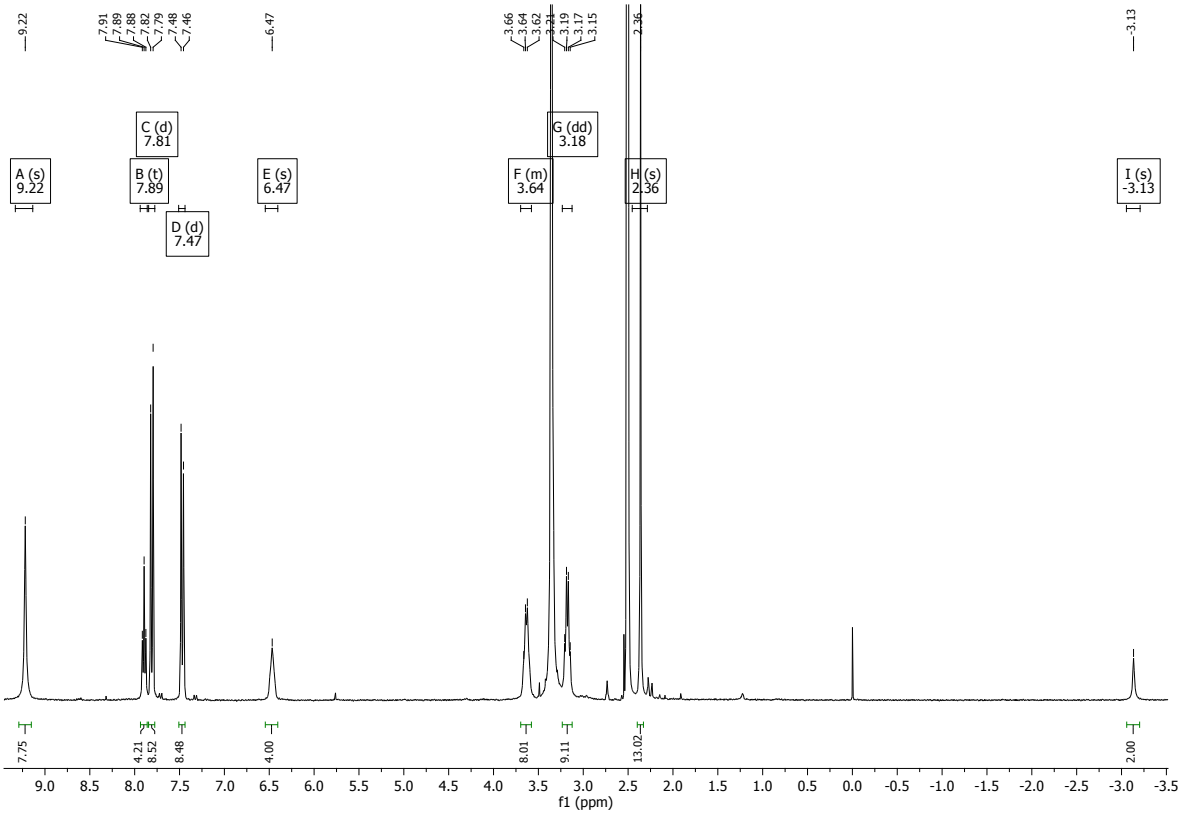

Figure SI 17: ^{1}H NMR spectrum of compound **2** in DMSO-d_6

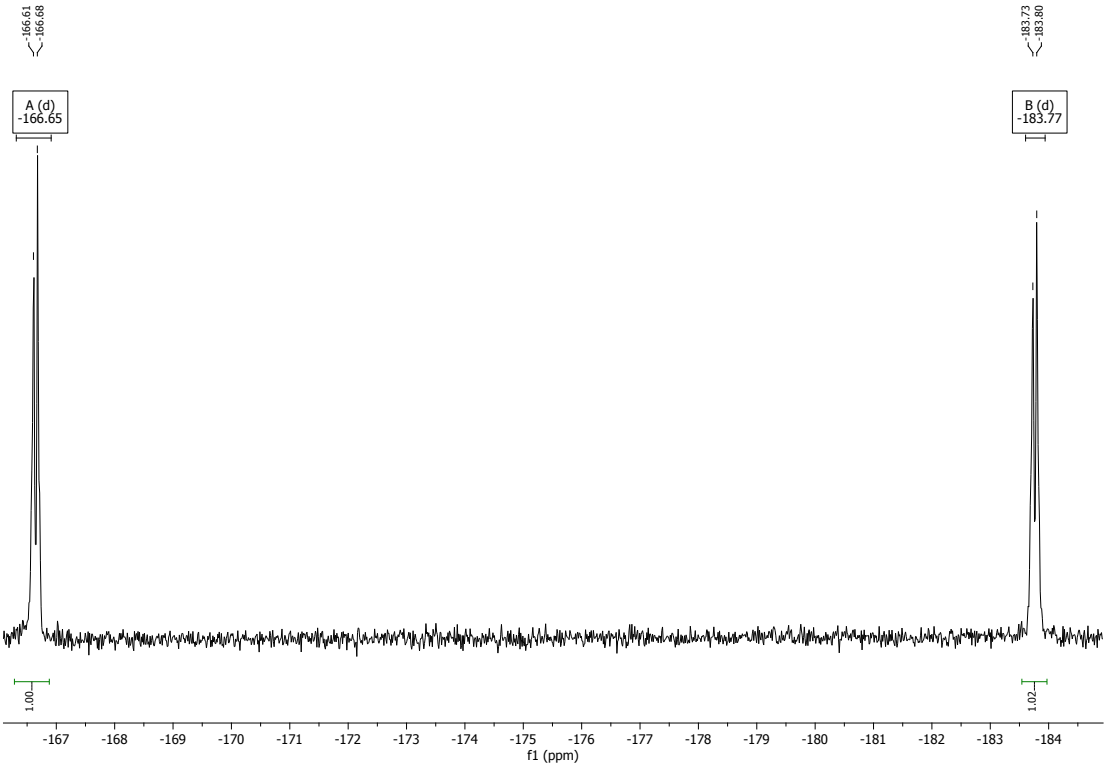

Figure SI 18: ^{19}F NMR spectrum of compound **2** in DMSO-d_6

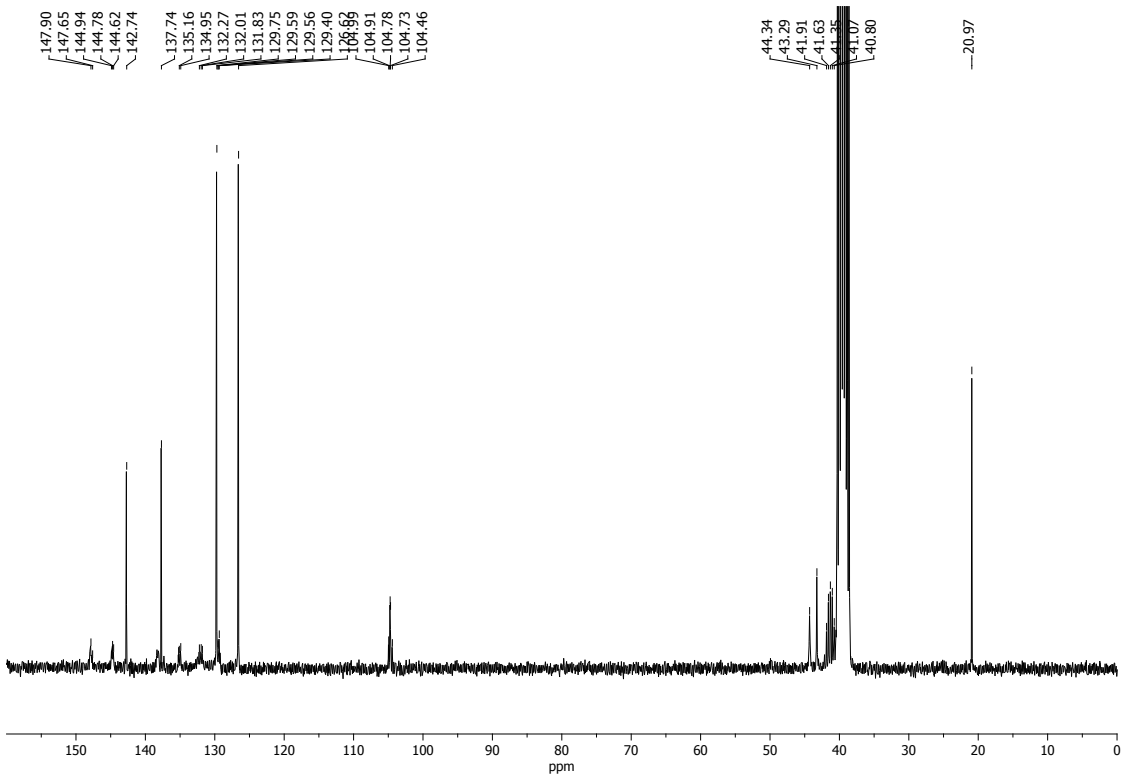

Figure SI 19: ^{13}C NMR spectrum of compound **2** in DMSO-d_6

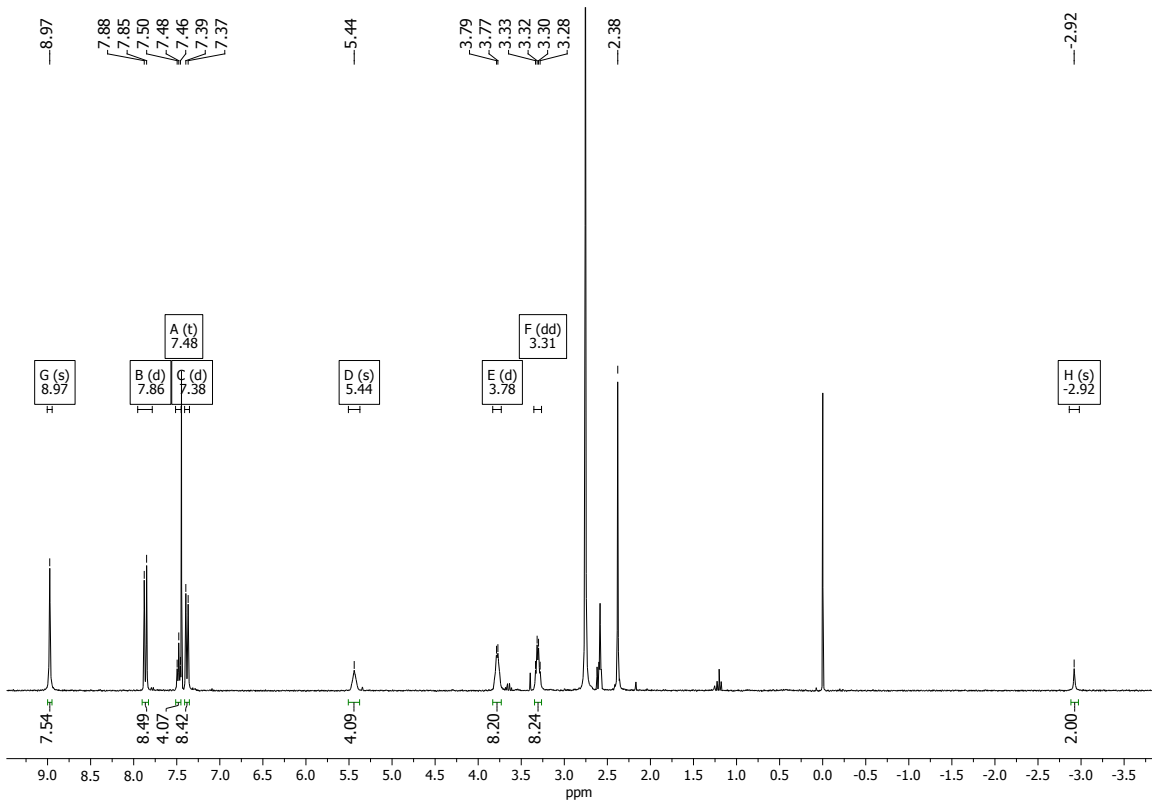

Figure SI 20: ^{1}H NMR spectrum of compound **2** in $CDCl_3$/DMSO-d_6

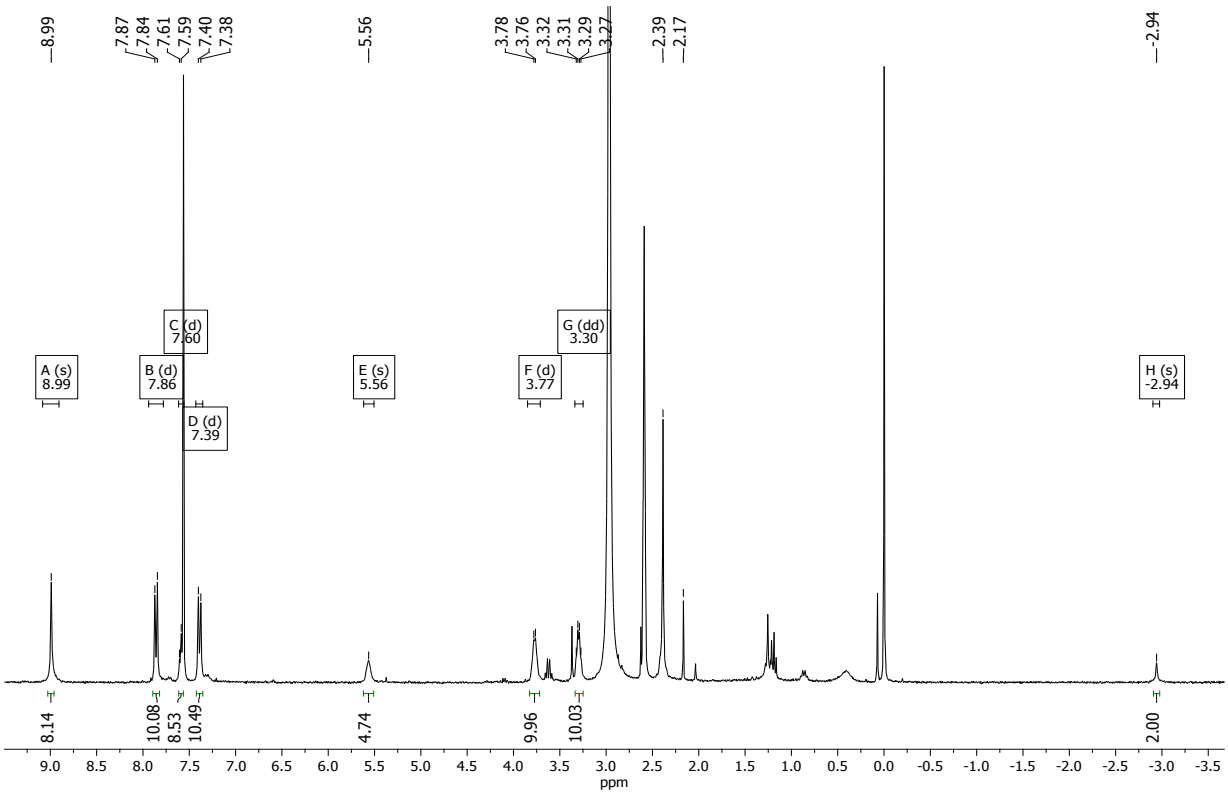

Figure SI 21: ^{1}H NMR spectrum of the protonated form of compound **2** in $CDCl_3$/DMSO-d_6; this species was generated *in situ* via the addition of 4 molar equiv. of acid; see experimental section.

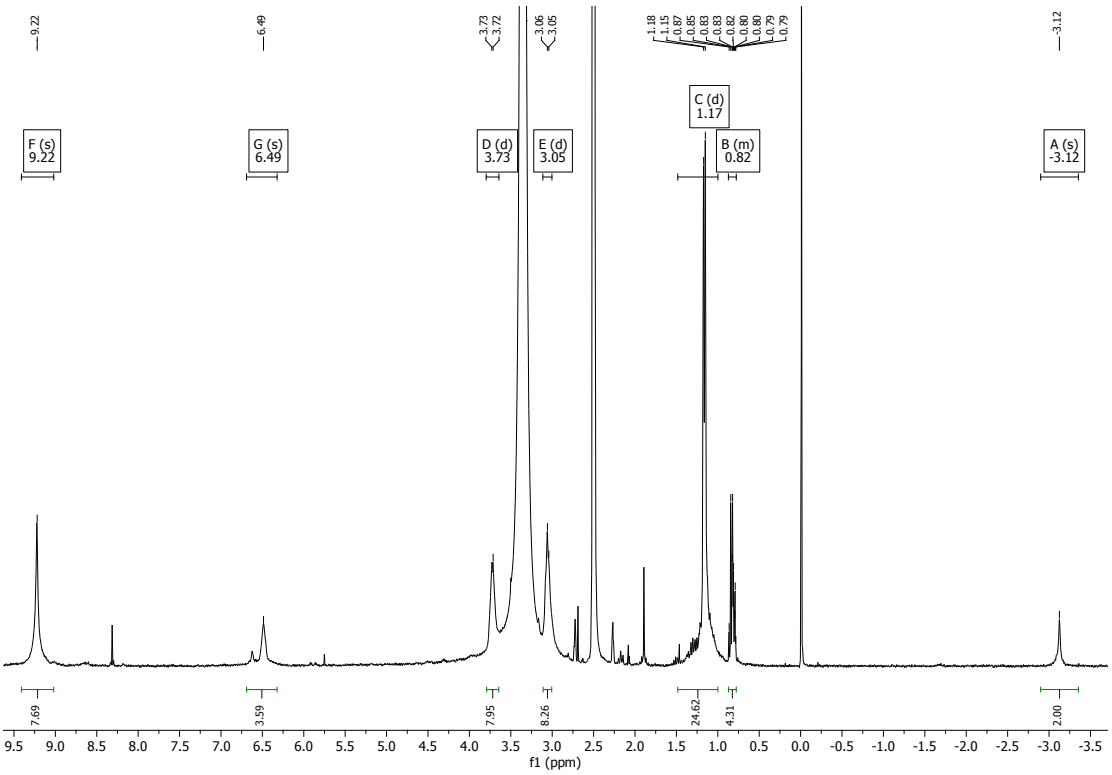

Figure SI 22: ^{1}H NMR spectrum of compound **3** in DMSO-d_6

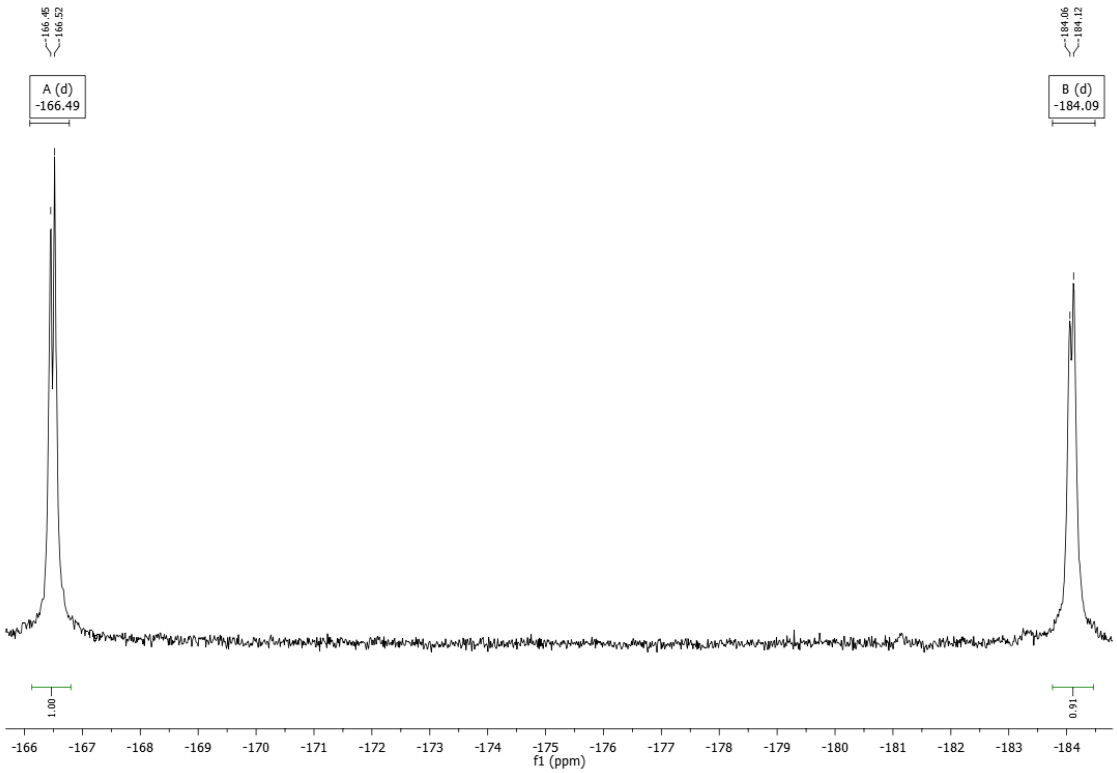

Figure SI 23: ^{19}F NMR spectrum of compound **3** in DMSO-d_6

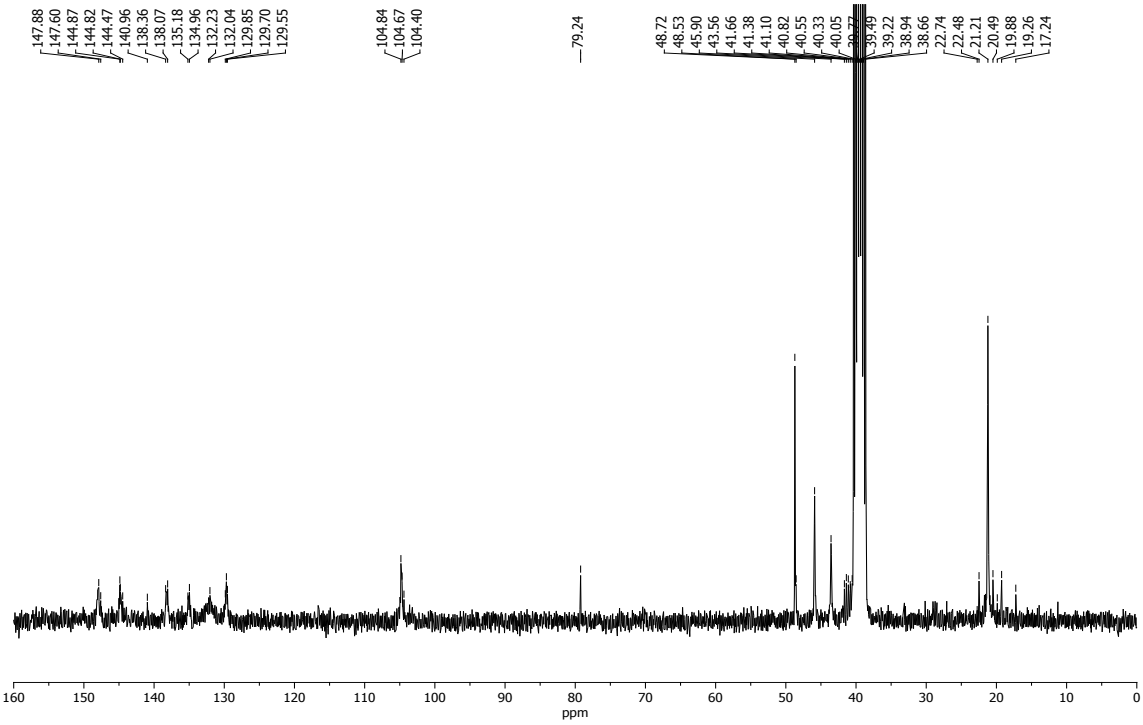

Figure SI 24: ^{13}C NMR spectrum of compound **3** in DMSO-d_6

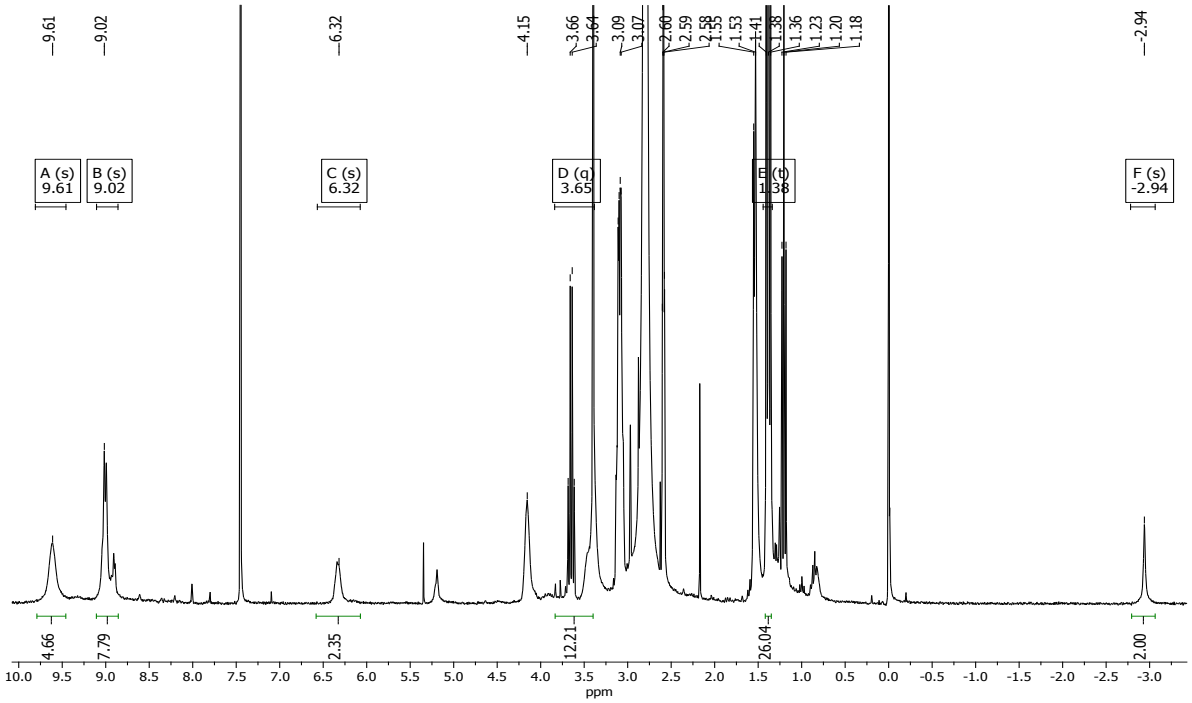

Figure SI 25: ^{1}H NMR spectrum of compound **3** in $CDCl_3$/DMSO-d_6

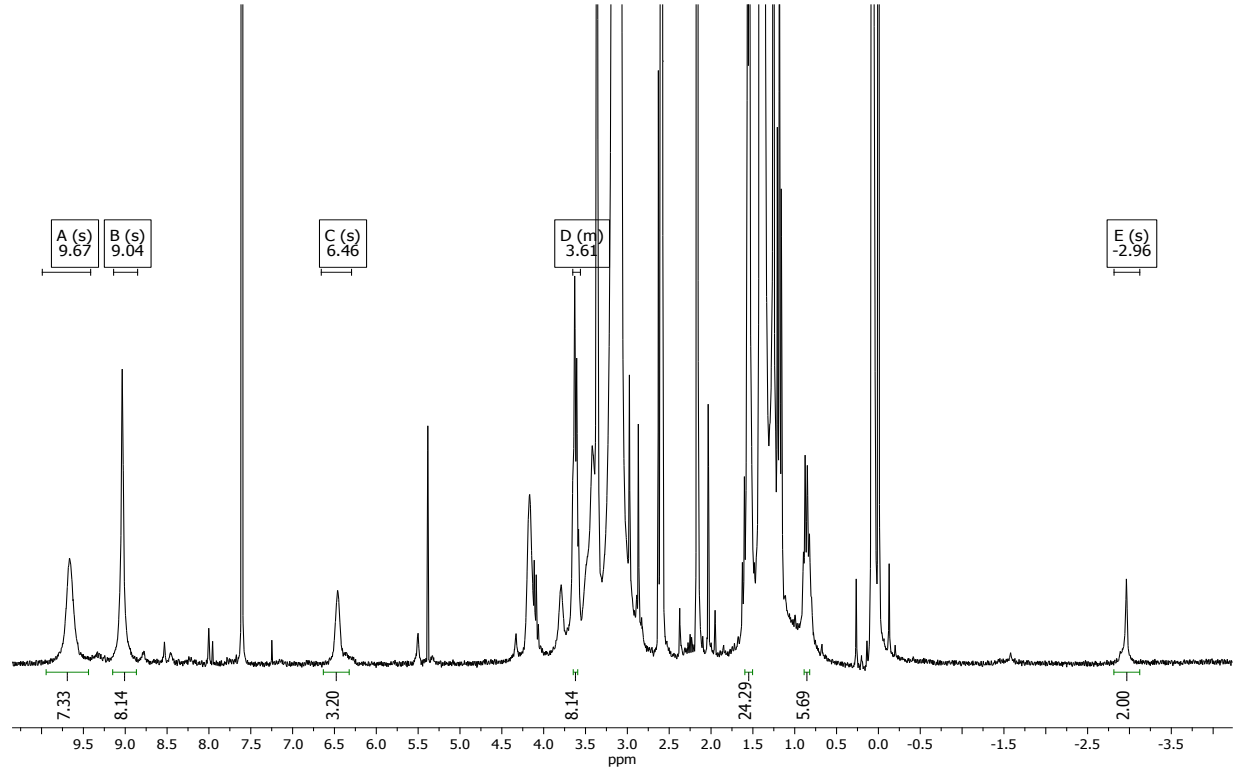

Figure SI 26: ^{1}H NMR spectrum of the protonated form of **3** in $CDCl_3$/DMSO-d_6; this species was generated via the addition of 4 molar equiv. of acid; see experimental section.

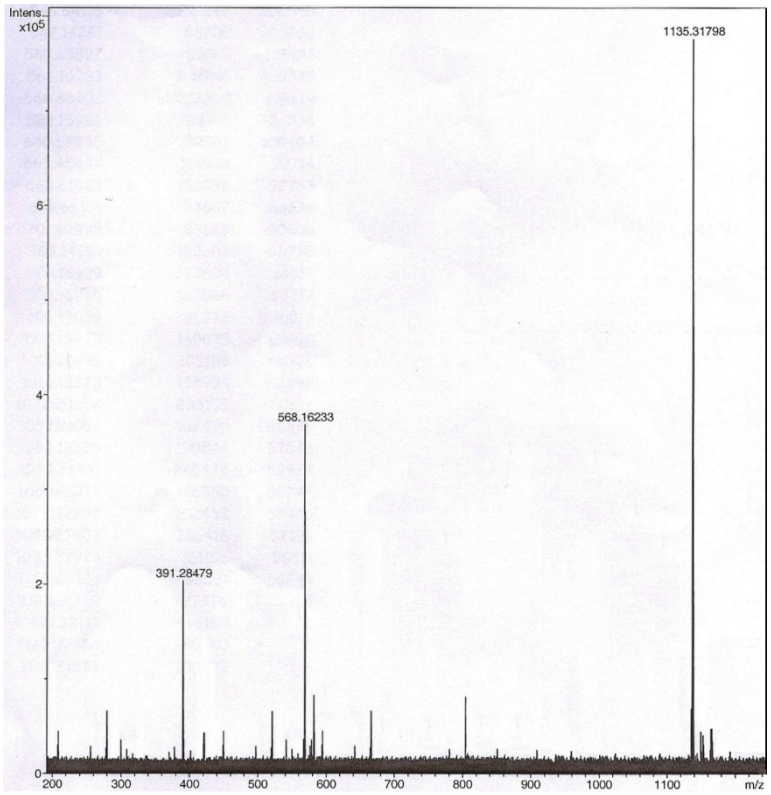

Figure SI 27: High resolution electrospray ionization mass spectrum (ESI MS) of compound **1**

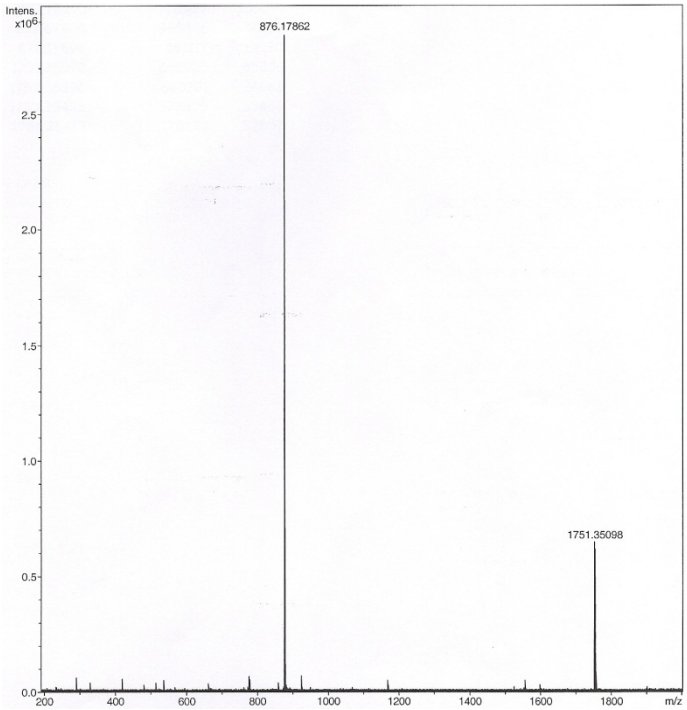

Figure SI 28: High resolution ESI MS of compound **2**

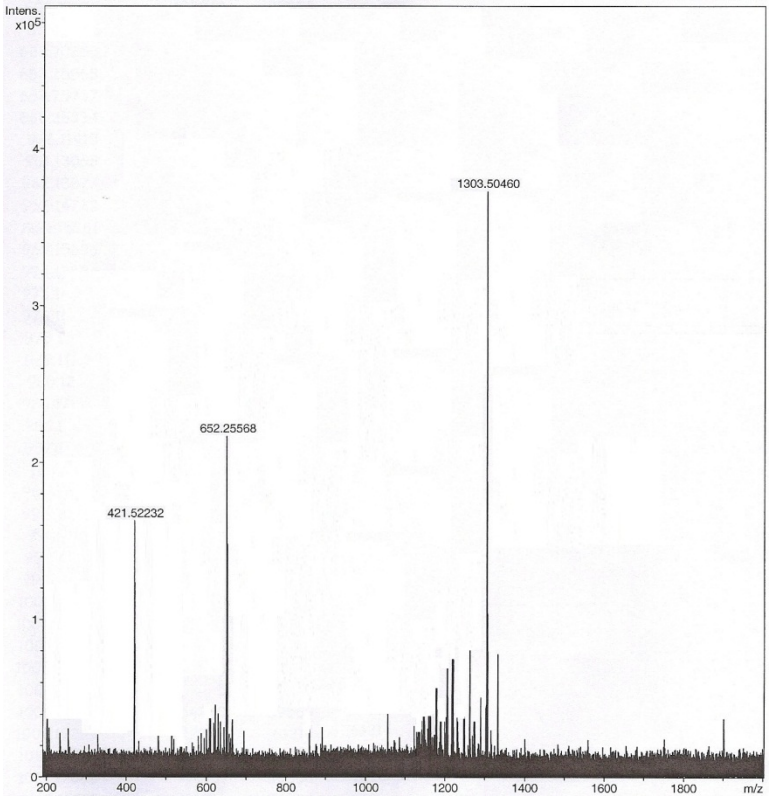

Figure SI 29: High resolution ESI MS of compound **3**

References

1 Connors, K. A. Binding Constants, The Measurement of Molecular Complex Stability; Wiley & Sons: New York, 1987

2 T. Kottke, D. Stalke, *J. App. Cryst*. 1993, **26**, 615.

3 APEX2, Data Collection Software Version 2.1-RC13, Bruker AXS, Delft, The Netherlands, 2006.

4 Cryopad, Remote monitoring and control, Version 1.451, Oxford Cryosystems, Oxford, United Kingdom, 2006.

5 SAINT+, Data Integration Engine v. 7.23a ©, 1997-2005, Bruker AXS, Madison, Wisconsin, USA.

6 Sheldrick, G. M. SADABS v.2.01, Bruker/Siemens Area Detector Absorption Correction Program, 1998, Bruker AXS, Madison, Wisconsin, USA.

7 Sheldrick, G. M. SHELXS-97, Program for Crystal Structure Solution, University of Göttingen, 1997.

8 Sheldrick, G. M. SHELXL-97, Program for Crystal Structure Refinement, University of Göttingen, 1997.

9 A. L. Spek, *Acta Cryst. A* 1990, **46**, C34.

10 A. L. Spek, *J. Appl. Crystallogr.* 2003, **36**, 7.

11 P. van der Sluis, A. L. Spek, *Acta Cryst. A* 1990, **46**, 194.